Zero-temperature criticality in a simple glass model

2000 J. Phys. A: Math. Gen. 33 465

(http://iopscience.iop.org/0305-4470/33/3/303)

J. Phys. A: Math. Gen. **33** (2000) 465–478. Printed in the UK PII: S0305-4470(00)06706-8

Zero-temperature criticality in a simple glass model

David Head

Department of Physics and Astronomy, University of Edinburgh, JCMB King's Buildings, Mayfield Road, Edinburgh EH9 3JZ, UK

E-mail: david@ph.ed.ac.uk

Received 6 August 1999

Abstract. We introduce the strongly interacting trap model, a version of Bouchaud's trap model for glasses (Bouchaud J-P 1992 *J. Physique* I **2** 1705). At finite temperatures the model exhibits glassy relaxation over intermediate timeframes but reaches a steady state at finite times. In the limit of zero temperature and with a suitably renormalized timescale the model maps onto the Bak–Sneppen model, widely studied in the context of self-organized criticality (Bak P and Sneppen K 1993 *Phys. Rev. Lett.* **71** 4083). Hence zero temperature is a critical point in all dimensions. These claims are supported by mean field analysis of the stationary solution and numerical simulations of a finite-dimensional lattice model.

1. Introduction

Our understanding of complex physical systems is often aided by the construction of simple mathematical models. A prime example from glass theory is the trap model of Bouchaud [1,2], which describes a system's relaxation purely in terms of activated processes between potential energy wells of various depths. With only a few assumptions the model manages to reproduce many of the phenomena commonly associated with glasses, such as a crossover to non-equilibrium behaviour as the temperature is lowered, and ageing in the low-temperature regime. Furthermore, the model is sufficiently generic to apply to structural as well as spin glasses, and has recently been extended to the study of rheology in glassy systems [3–6].

However, there are a number of spin-glass models that exhibit a continuous phase transition, or critical point, in the limit of zero temperature, quite unlike the current realization of Bouchaud's trap model. These include Stein and Newman's model, which maps onto invasion percolation at a temperature $T = 0$ [7, 8]; the two-dimensional Ising spin glass [9]; and the Sherrington–Kirkpatrick model under infinitesimal variations of the external magnetic field [10].

In this paper we introduce a modified version of Bouchaud's trap model which incorporates a form of interaction between different subsystems. It is shown that in the limit of zero temperature this model maps onto a self-organized critical system known as the Bak–Sneppen model [11,12], so $T = 0^+$ is a critical point in all dimensions, including the infinite-dimensional mean field model. Although the Bak–Sneppen model was originally devised to explain the pattern of evolutionary bursts in the fossil record known as 'punctuated equilibria', it was justified in terms of activated processes over (fitness) barriers and so its biological interpretation is purely semantic.

This paper is arranged as follows. In section 2, Bouchaud's model is briefly reviewed before the new model is defined in its mean field form. The corresponding master equation is

0305-4470/00/030465+14$30.00

solved in the steady state. The relationship with the Bak–Sneppen model implies that the model can also be defined on a lattice, and this modification is studied numerically in section 3. The simulations were also employed to check the analytical predictions of the mean field equations. Finally, our work is summarized in section 4.

2. Definition of the mean field model and the stationary solution

In Bouchaud's formalism, the state of the system is represented by a particle (or many particles, if the system is treated as a collection of subsystems) moving in configuration space over an energy landscape, which is 'rugged' in the sense that most of the particle's time is spent trapped in potential wells or 'traps' [1, 2]. Motion within traps is not explicitly incorporated; instead, it is simply assumed that whatever dynamics is present gives rise to an activation probability that depends on the barrier height b and the temperature T according to the Arrhenius form $\omega_0 \mathrm{e}^{-b/T}$, where ω_0 fixes the timescale.

When a particle is activated it 'hops' to a new trap, where it remains until it is again activated by thermal fluctuations. Thus the state of the system can be described by the probability $P(b, t)$ that it is in a trap of depth b at time t (in the many-particle interpretation, $P(b, t)$ is the distribution of barriers in all the subsystems). Given that the barrier heights are distributed according to some *prior* distribution $\rho(b)$, then $P(b, t)$ evolves according to the master equation

$$\frac{1}{\omega_0}\frac{\partial P(b,t)}{\partial t} = -\mathrm{e}^{-b/T}P(b,t) + \omega(t)\rho(b) \tag{1}$$

where $\omega_0\omega(t)$ is the total rate of hopping at time t,

$$\omega_0\omega(t) = \omega_0 \int_0^\infty \mathrm{e}^{-b/T}P(b,t)\,\mathrm{d}b. \tag{2}$$

The first and second terms on the right-hand side of (1) correspond to hopping out of and into traps of depth b, respectively. For simplicity is has been assumed that $\rho(b)$ is independent of t and T, and barrier heights before and after a hop are uncorrelated.

When a steady state solution of (1) exists, it takes the form

$$P_\infty(b) \equiv \lim_{t\to\infty} P(b,t) = \omega_\infty \mathrm{e}^{b/T}\rho(b) \tag{3}$$

using $\omega_\infty = \lim_{t\to\infty}\omega(t)$. For a prior distribution with an exponential tail $\rho(b) \sim \mathrm{e}^{-b/b_0}$ (which may be generic to glassy systems [2]), $P_\infty(b)$ can only be normalized for $T > b_0$, when it takes the form of a Boltzmann distribution. No normalizable steady state solution exists for $T \leqslant b_0$, when the system perpetually evolves into deeper and deeper traps. In this manner the model exhibits a phase transition from equilibrium to non-equilibrium behaviour at $T = b_0$, i.e. a *glass* transition.

2.1. Master equation for strong interactions

Although the basic trap model described above exhibits a simple and elegant glass transition, it has the undesirable feature that the mean barrier height diverges with time when $T \leqslant b_0$. This suggests that there may be some mechanism currently lacking from the model which eventually halts its progression into ever deeper traps. For instance, it is known that the system will equilibrate at very long times if it can only sample a finite number of different configurations [1]. Here we argue that introducing a suitable form of interaction between the subsystems can achieve a similar effect.

Bouchaud *et al* have considered the effect of allowing each hop to slightly alter the barriers of other subsystems [13], so we are now working strictly in the many-particle interpretation. In their scheme, the barrier distribution $P(b, t)$ is perturbed at a rate proportional to the overall hopping rate $\omega(t)$, giving rise to an extra term in the master equation (1) of the form

$$\omega(t) \int_0^\infty \mathcal{T}(b' - b)(P(b', t)\rho(b) - P(b, t)\rho(b'))\, \mathrm{d}b'. \tag{4}$$

For weak interactions, $\mathcal{T}(b)$ is narrow and (4) reduces to a diffusion-like term which was shown to not alter the essential nature of the glass transition [13].

Here we consider the opposite extreme of a broad $\mathcal{T}(b) \equiv z$, where z is a constant. This corresponds to a form of *strong* interaction in which every hopping subsystem causes z other subsystems to have their barriers assigned *entirely* new values. This erases the memory of the system at a rate $z\omega(t)$ and, as shall be demonstrated below, ultimately removes the glass transition. Subsystems with very large barriers that would not normally hop until very late times will now interact instead, which on average lowers their barriers towards the mean of $\rho(b)$ and allows them to hop much earlier than they would in the absence of strong interactions. Thus the interactions introduce a form of *dynamically generated cut-off* into the system.

It is straightforward to integrate (4) with $\mathcal{T}(b) = z$ to give the new master equation

$$\frac{1}{\omega_0}\frac{\partial P(b, t)}{\partial t} = -\mathrm{e}^{-b/T} P(b, t) + \omega(t)\rho(b) + z\omega(t)(\rho(b) - P(b, t)) \tag{5}$$

with the definition of $\omega(t)$ unchanged from (2). The steady state solution of (5) is non-Boltzmann,

$$P_\infty(b) = \frac{z+1}{z}\left(1 + \frac{\mathrm{e}^{-b/T}}{z\omega_\infty}\right)^{-1} \rho(b) \tag{6}$$

so $P_\infty(b) \sim \rho(b)$ as $b \to \infty$ for all T, i.e. $P_\infty(b)$ is always normalizable when $z > 0$. This suggests that there is no true finite temperature glass transition, although it has yet to be shown that the system always approaches this stationary solution. Numerical evidence that this is indeed the case is presented in section 3, where it is also argued that glassy behaviour may persist over intermediate timeframes at low temperatures. For the remainder of this section we restrict our attention to analysis of the stationary solution (6).

2.2. Steady state solution

For the case of a simple exponential prior $\rho(b) = \frac{1}{b_0}\mathrm{e}^{-b/b_0}$, it is possible to derive an exact expression for ω_∞ for $z > 0$. Details of this calculation are given in appendix A; here we just quote the final result. In terms of the *reduced temperature* $x = T/b_0$, the expression for ω_∞ is

$$(z\omega_\infty)^x + \frac{\sin \pi x}{\pi x}\left\{\frac{1}{z+1} + x\sum_{k=0}^{\infty}\frac{(-z\omega_\infty)^k}{k-x}\right\} = 0. \tag{7}$$

It may at first appear that the factor of $\sin \pi x$ on the left-hand side of (7) would imply that $\omega_\infty \to 0$ for integer values of x. However, there is also a simple pole in the sum for such x, and in fact these two effects cancel. The equivalent expression to (7) for integer x is

$$\frac{(z\omega_\infty)^{-x}}{x(z+1)} = (-1)^x \ln\left(1 + \frac{1}{z\omega_\infty}\right) + \sum_{k=0}^{x-1}\frac{(-1)^k (z\omega_\infty)^{k-x}}{x-k}. \tag{8}$$

The numerical plot of (7) and (8) given in figure 1 confirms the monotonic dependence of ω_∞ on temperature.

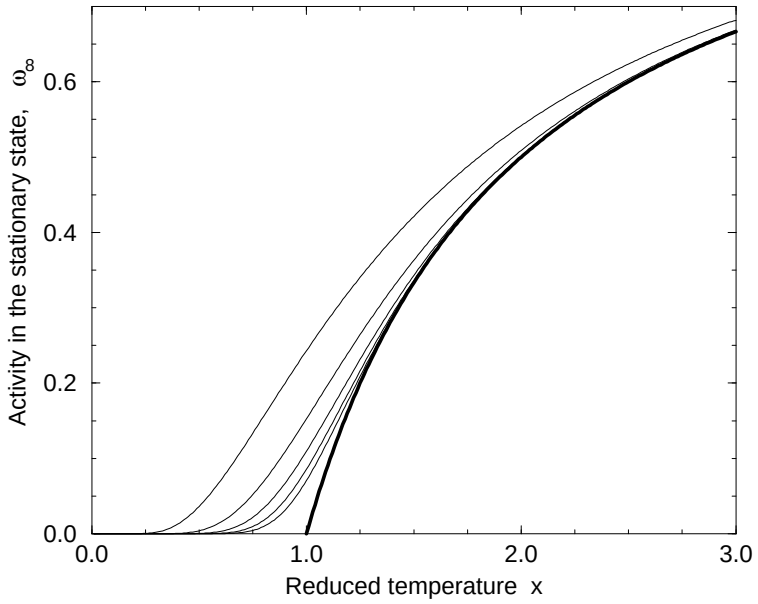

Figure 1. Plot of ω_∞ against the reduced temperature $x = T/b_0$, found from (7) and (8) by the method of interval bisection. From top the bottom, the thin curves refer to $z = 10^{-1}$, 10^{-2}, 10^{-3}, 10^{-4} and 10^{-5}, respectively. For comparison the $z \equiv 0$ solution $\omega_\infty = 1 - 1/x$ is plotted as a thick curve.

One might expect that $P_\infty(b)$ for small z could be expressed as just an $\mathcal{O}(z)$ perturbation around the $z \equiv 0$ solution given in (3). In fact this is only true for temperatures $x > 2$, as we now demonstrate. As $z \to 0$, (7) can be expanded in powers of z and the higher-order terms dropped. The identification of the leading-order term depends upon the value of x. For $x > 1$, the leading-order term is $\mathcal{O}(z\omega_\infty)$ and

$$\omega_\infty = \left(1 - \frac{1}{x}\right)(1 + \mathcal{O}(z)) \tag{9}$$

which is just an $\mathcal{O}(z)$ perturbation around the original solution (3). This is not true for $x < 1$, when the $(z\omega_\infty)^x$ term is now leading order and

$$\omega_\infty \approx \left(\frac{z}{z+1}\right)^{\frac{1}{x}-1} \left(\frac{\sin \pi x}{\pi x}\right)^{\frac{1}{x}}. \tag{10}$$

This holds as long as the $\mathcal{O}(z\omega_\infty)^x$ term is much larger than the $\mathcal{O}(z\omega_\infty)$ term, which corresponds to $z^{1-x} \ll 1$. This should be contrasted to the original model, where ω_∞ is not even defined for $x \leqslant 1$. Repeating this procedure for integer x produces the same expression as (9) for $x \geqslant 2$ and $\omega_\infty \sim -(\ln z)^{-1}$ for $x = 1$.

The consequence of having $z > 0$ becomes apparent at higher temperatures if one considers the distribution of barriers as a whole, rather than just ω_∞. By substituting (9) into the expression for $P_\infty(b)$ given in (6) and expanding in powers of z, one readily sees that $P_\infty(b)$ can only be expressed as an $\mathcal{O}(z)$ perturbation around the original solution when $x > 2$; for $x \leqslant 2$, the assumption of a linear expansion breaks down. This higher-temperature divergence can be explained by observing that, when $z \equiv 0$, the mean time between hops diverges in the stationary state for $x \leqslant 2$ [2]. In contrast, when $z > 0$ the mean time between interactions approaches $(z\omega_\infty)^{-1}$, which is *always* finite. Thus the interactions will always be significant when $x \leqslant 2$, no matter how small z may be.

2.3. Solution at the critical point $T = 0^+$

An important consequence of introducing this new form of interaction is that the system now becomes critical in the limit $T \to 0^+$. This can be most clearly seen by considering a finite system of N subsystems with barriers b_i, $i = 1 \ldots N$. For small T the system will remain static for long periods, but when a subsystem *does* eventually hop, the probability that it had the barrier b_i is

$$p_i = \frac{\mathrm{e}^{-b_i/T}}{\sum_{j=1}^{N} \mathrm{e}^{-b_j/T}}. \tag{11}$$

Since the system is finite it is always possible to identify a unique minimum barrier $b_{\min}$ (assuming that $\rho(b)$ does not contain any delta-function peaks). Suppose it is subsystem j that has the barrier $b_{\min}$, then inspection of (11) shows that $p_j \to 1$ as $T \to 0^+$, while $p_i \to 0$ for all $i \neq j$. Thus the identification of the activated subsystem is entirely deterministic—it is *always* the one with the smallest barrier. This is now algorithmically identical to the Bak–Sneppen model, already widely studied in the context of self-organized criticality [11, 12]. Hence $T = 0^+$ is a critical point of the current model. Note that the timescale in the Bak–Sneppen model is normalized to precisely one hop per unit time, whereas in our model the time between hops can vary. However, as explained below, the maximum time between hops is of the order of $\mathrm{e}^{b_c/T}$ with b_c constant, which is finite for all $T > 0$. Hence we do not anticipate any problems with, e.g., diverging moments of the distribution of hopping times.

The Bak–Sneppen model is usually defined on a lattice, in which interactions only occur between nearest neighbours. This suggests that the current model can also be given a lattice interpretation, and this modification is considered in section 3. However, a mean field solution to the Bak–Sneppen model already exists [14, 15], which should be the same as the $T \to 0^+$ solution of the current model. This indeed proves to be the case for the stationary distribution $P_\infty(b)$, derived in appendix B for arbitrary $\rho(b)$,

$$P_\infty(b) \approx \frac{z+1}{z} \frac{\rho(b)}{1 + \mathrm{e}^{(b_c - b)/T}} \qquad \text{for small } T \tag{12}$$

$$\sim \frac{z+1}{z} \theta(b - b_c)\rho(b) \qquad \text{as } T \to 0^+ \tag{13}$$

where $\theta(x)$ is the usual theta function and b_c is defined by

$$\int_0^{b_c} \rho(b)\,\mathrm{d}b = \frac{1}{z+1}. \tag{14}$$

This is also the mean field solution to the Bak–Sneppen model, to within $\mathcal{O}(1/N)$. Note that (12) was found by taking $T \to 0^+$ *after* taking the thermodynamic limit $N \to \infty$. That it agrees with the mean field solution of the Bak–Sneppen model, which corresponds to taking $T \to 0^+$ *before* $N \to \infty$, suggests that the order of the limits may not be important for time-independent quantities, although this may not hold for time-dependent measures.

The discontinuity in b in (13) arises from the existence of a single characteristic time between interactions of the order of $\omega_0 \mathrm{e}^{b_c/T}$. The expected time until a subsystem with a barrier b hops is $\omega_0 \mathrm{e}^{b/T}$, so subsystems with $b \ll b_c$ will almost certainly hop before interacting, whereas those with $b \gg b_c$ will almost certainly interact before hopping. Only barriers $b \approx b_c$ will have comparable probabilities of either hopping or interacting. As T is lowered the distribution of hopping times becomes extremely broad, corresponding to an increasingly narrow range of b for which the rates of hopping to interaction are comparable, eventually collapsing onto the single point b_c at $T = 0^+$. Since hopping takes place over timescales much shorter than interactions, there will only be a vanishingly small proportion of subsystems with $b < b_c$ at any given time, as implied by the theta function in (13).

This suggests the classification of subsystems as either 'active' (those with $b < b_c$) or 'inactive' (those with $b > b_c$). In this heuristic scheme, active subsystems may become inactive by hopping into a trap with a barrier greater than b_c, but inactive subsystems can only become active via interactions. This description is somewhat reminiscent of the contact process, a critical model which falls into the universality class of directed percolation [16]. However, the contact process only becomes critical when its control parameter is set to some finite value—in effect, its value of b_c has to be set 'by hand'. In contrast, the current model automatically finds b_c in the limiting case $T \to 0^+$. It is in this sense that the Bak–Sneppen model can be said to be 'self-organized' critical. A fuller discussion of the relationship between this model and self-organized criticality will be made elsewhere [17]. Note that the Bak–Sneppen model and the contact process have different driving terms and fall into different universality classes†.

3. Finite-dimensional lattice model

The analysis of the preceeding section is mean field in the sense that the interactions have been assumed to act homogeneously throughout the system. In this section the model is given spatial definition by identifying each subsystem with a single site of a d-dimensional lattice. The subsystems become thermally activated as before, but now each activation event can only alter the barriers of adjacent lattice sites, so the interactions are strictly short-ranged. Only a one-dimensional lattice is considered here, but the model can be defined in higher dimensions in a similar manner.

The lattice model is defined as follows. A single barrier height b_i is stored in each site $i = 1 \ldots N$ of a one-dimensional lattice of size N, with initial conditions to be specified below. At the start of each time step, every site is checked to see whether it becomes activated, which it does with a probability $\mathrm{e}^{-b_i/T}$. Any activated subsystems hop to a new trap with a new barrier b_i drawn from $\rho(b)$. Furthermore, the barriers in the adjacent sites b_{i-1} and b_{i+1} are also assigned new values—this represents the strong interactions. Note that in these scheme each site hops at most once per time step. This discrete time variable differs from the continuous time employed in the mean field equations in section 2, but should make little difference when the overall rate of activity is low.

Thus every activation event causes *three* barriers to change value—the activated site itself, and the barriers in both of the adjacent sites. This would appear to fix $z = 2$. However, smaller values of z can be incorporated by stipulating that b_{i-1} and b_{i+1} only change values with a probability $z/2$, where now $0 \leqslant z \leqslant 2$. Simulation results for various z and T are discussed in sections (3.1) to (3.3) below. Periodic boundary conditions have been assumed throughout, so $b_{N+1} \equiv b_1$. The prior distribution was taken to be the simple exponential $\rho(b) = \frac{1}{b_0}\mathrm{e}^{-b/b_0}$. Care was also taken to ensure that the supplied random number generator gave good statistics deep in the tail of an exponential distribution.

3.1. Existence of a stationary solution

The simulations were first employed to see whether or not there exists a stationary solution in the lattice model, and if so, how robust it is with respect to the initial conditions. To test this, two very different initial configurations were used. The first was an initial 'quench' where all the b_i were drawn from $\rho(b)$ but spatially uncorrelated. These runs were then repeated with the same parameters but starting with every b_i arbitrarily large except for a single 'seed' at the origin with $b_0 = 0$ (or any finite value). In both cases the barrier distribution $P(b, t)$ appeared

† The contact process also has slightly different interaction terms to the Bak–Sneppen model, but these can be altered without changing its universality class [18, 19].

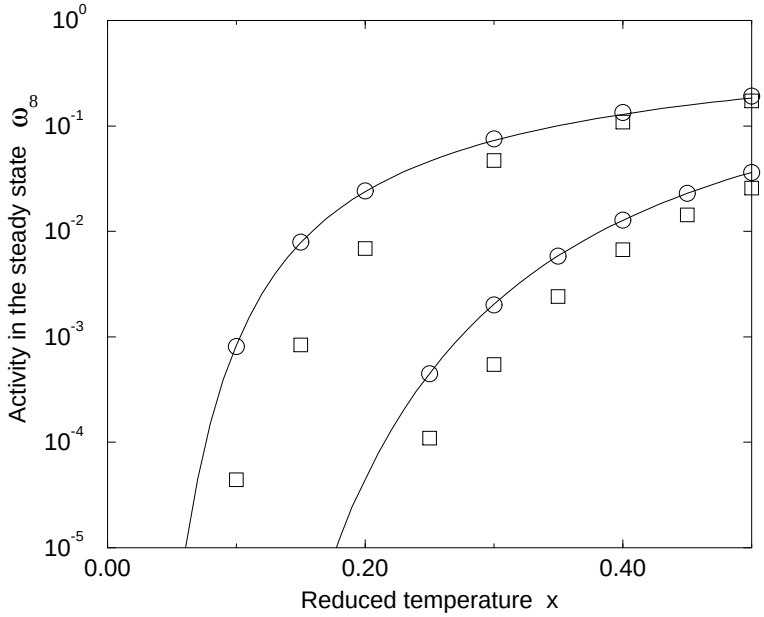

Figure 2. Plot of ω_∞ against x for $z = 1$ (upper data sets) and $z = 0.1$ (lower data sets). In both cases, the circles and squares correspond to simulation results for the RNN and one-dimensional models, respectively. The system size was $N = 10^4$ and the estimated error bars are smaller than the symbols. The solid curves are the mean field predictions from (7) and (8).

to converge to the same distribution $P_\infty(b)$, which remained steady within the timeframe of the simulations, typically 10^7 time steps (although the situation is not so clear for the $T = 0^+$ limit in low dimensions; see section 3.3). Since the initial conditions were so very different, it seems likely that this same distribution is approached irrespective of the initial state. The stationarity of this solution is confirmed in section 3.2.

Although it has already been shown that the mean field equations of section 2.1 admit a stationary solution, it is by no means clear that it is always, if ever, reached. To investigate this, the simulations were also repeated using a 'random nearest-neighbour' (RNN) algorithm in which the neighbours of the hopping sites are chosen entirely at random from the remainder of the system, with new neighbours being chosen at every time step. Apart from finite size effects and the discrete time variable, this should behave identically to the mean field model. Simulations of the RNN model show that the same stationary solution was reached for both sets of initial conditions, as in the one-dimensional case. Furthermore, the numerical estimate of ω_∞ was found to agree well with the theoretical predictions (7) and (8), as plotted in figure 2.

Also plotted in figure 2 are the equivalent values of ω_∞ for the one-dimensional model, which consistently lie under the mean field values. This is because the interactions are now spatially correlated with the hopping sites and are more likely to occur in regions of high activity, i.e. low barriers. Since the interactions tend to decrease barrier values towards the mean of $\rho(b)$, their effect on $P(b, t)$ will be *weaker* in the one-dimensional model than the corresponding mean field system. Thus the stationary state will not be reached until much later times, when the activity will have decayed to smaller values, as in figure 2. In the $T \to 0^+$ limit the limiting activity is $\omega_\infty \sim \mathrm{e}^{-b_c/T}$ (see appendix B), so as a corollary b_c should be *higher* in lower dimensions, and indeed this has already been observed in the Bak–Sneppen model [14, 15].

3.2. Interruption of ageing

An important feature of many glassy systems is that their behaviour depends upon the time since the initial quench, a property known as 'ageing'. This phenomenom can be quantified by use of the two-time correlation function $C(t_w + t, t_w)$, defined here as the proportion of sites that have not hopped between times t_w and $t_w + t$ following a quench at $t = 0$. In Bouchaud's model the system becomes *time-translationally invariant* above the glass transition, i.e. $C(t_w+t, t_w) \to C_{eq}(t)$ as $t_w \to \infty$ when $x > 1$. In contrast, when $x < 1$ the system behaviour cannot be decoupled from t_w and instead one finds $C(t_w + t, t_w) \to C_{neq}(t/t_w)$, demonstrating that the system ages [2].

To confirm that the simulations do indeed converge to a stationary solution, it is necessary to show that $C(t_w + t, t_w)$ converges to a time-translationally invariant solution $C_\infty(t)$. This has been checked in both one-dimensional and RNN simulations, and in all cases stationarity was reached after waiting times $t_w \gg t_{ia}$, where t_{ia} depends on z, T and the dimensionality. A typical example is given in figure 3. An estimate of t_{ia} for low temperatures in the mean field can be found by following the procedure described in [2]. This involves substituting the trial solution

$$P(b, t) = \frac{1}{T} u\phi(u) \tag{15}$$

expressed here in terms of the dimensionless variable $u = \frac{1}{\omega_0 t} e^{b/T}$. For $\rho(b) = \frac{1}{b_0} e^{-b/b_0}$ master equation (5) then becomes

$$u^2 \frac{d\phi(u)}{du} + (u - 1)\phi(u) = \left(\int_{1/\omega_0 t}^{\infty} \frac{\phi(v)}{v}\, dv \right) \left(zu\phi(u) - \frac{x(1+z)}{(\omega_0 u t)^x} \right) \tag{16}$$

where the integral is just $\omega(t)$ expressed in terms of ϕ and u. Dimensional analysis suggests that the first term on the right-hand side of (16) can be neglected for small t. This allows a t-independent scaling solution to be found which exhibits ageing [2]. However, if $z > 0$ then, as $t \to \infty$, the second term will become negligible and it is straightforward to show that no self-consistent scaling solution exists. From this we infer that the ageing is *interrupted* at some finite time. The crossover time t_{ia} corresponds to times when both terms are of comparable magnitude, which can be estimated by dimensional analysis to be

$$t_{ia} \sim \left(\frac{1 + z}{z} \right)^{1/x} \sim e^{b_c/T} \tag{17}$$

where b_c is the same as that defined in (14). Note that t_{ia} diverges rapidly as $T \to 0$, so ageing behaviour may persist over intermediate (possibly experimental) timeframes at low temperatures.

3.3. Ageing in the $T = 0^+$ limit

The analysis of the $T = 0^+$ limit presented in section 2.3 was limited to the stationary barrier distribution $P_\infty(b)$. We now turn to consider time-dependent behaviour, which requires careful consideration of the choice of timescale. Clearly, as $T \to 0^+$ the rate of hopping in a finite system becomes vanishingly small and so the timescale must be normalized in some manner to attain non-trivial behaviour. Two different timescales will be considered here. The first is the *event timescale* τ in which precisely one subsystem from a total of N hops per unit τ. This is the usual choice in the Bak–Sneppen model. The second time variable we shall consider is the *avalanche timescale* τ^{av}, defined such that τ^{av} increases by one unit for every avalanche in the system, where an avalanche is defined below. Although not usually considered in connection with the Bak–Sneppen model, τ^{av} is more in line with the timescale employed in,

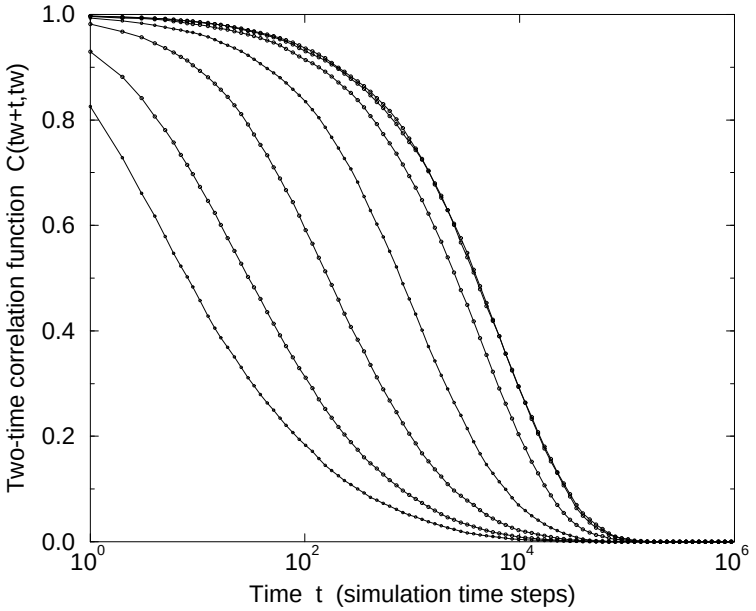

Figure 3. The two-time correlation function $C(t_w + t, t_w)$ plotted against t for a one-dimensional lattice with $N = 10^4$, $z = 0.1$, $x = 0.35$ and $\omega_0 = 1$. From left to right, $t_w = 10^0$, 10^1, 10^2, 10^3, 10^4, 10^5 and 10^6. Note that the last two curves overlap. The system was started from an initial quench with the b_i drawn from $\rho(b)$ and uncorrelated.

e.g., the sandpile model [20]. The existence of ageing behaviour depends crucially upon which timescale is adopted, as we now demonstrate.

Boettcher *et al* have found that the Bak–Sneppen model exhibits a form of ageing in one- and two-dimensional simulations starting from a single active seed [21, 22]. We have adapted our code to employ event time in simulations starting from an initial quench and have also observed ageing in the one-dimensional model, but *not* in the RNN model. Results from the one-dimensional simulations are given in figure 4, which appears to exhibit ageing for the longest times we were able to simulate, up to $\tau_w = 10^8$ on a $N = 2 \times 10^4$ lattice, although the statistics become very noisy at later times. For large τ_w the data shows some indications of collapse onto a scaling function $C_\infty(\tau/\tau_w)$, as demonstrated in figure 5. In contrast the results from the RNN simulations (not given) fail to exhibit any form of ageing whatsoever.

It is possible to provide a rough derivation of the ageing behaviour observed in our simulations by considering the pattern of activity of hopping sites as the system evolves from its initial quench. This argument employs known results for the Bak–Sneppen model, which we do not attempt to justify here; the reader is instead referred to [12] for a complete description. Initially, the location of the hopping site moves around the system at random, but as τ increases it tends to repeatedly visit one part of the system for a finite time before jumping to another, uncorrelated region. These localized spatiotemporal regions of activity are known as *avalanches*. The expected duration of the avalanche $\langle S \rangle$ and the expected number of sites covered during the avalanche $\langle n_{\rm cov} \rangle$ diverge with time according to [12]

$$\langle S \rangle \sim \left(\frac{\tau}{N}\right)^{\frac{\gamma}{\gamma-1}} \tag{18}$$

$$\langle n_{\rm cov} \rangle \sim \left(\frac{\tau}{N}\right)^{\frac{1}{\gamma-1}} \tag{19}$$

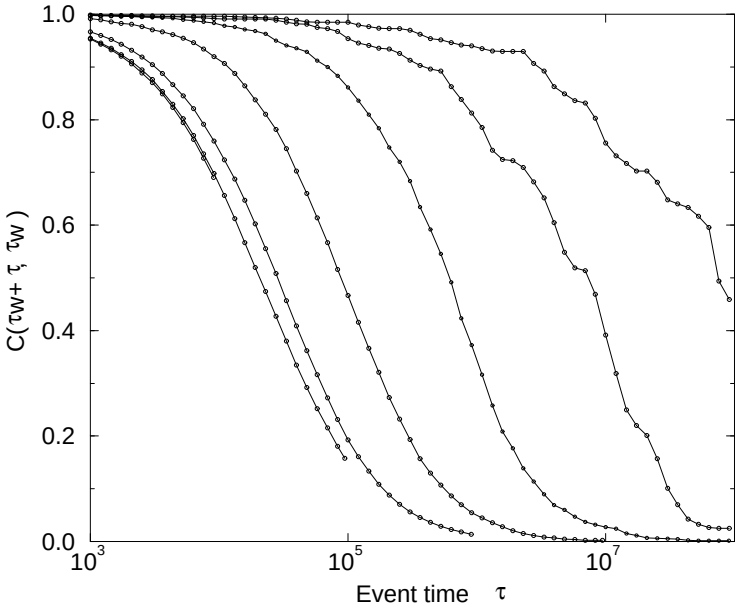

Figure 4. $C(\tau_w+\tau, \tau_w)$ versus τ for a one-dimensional lattice of $N = 2 \times 10^4$ sites in the $T \to 0^+$ limit in event time τ, making this identical to the Bak–Sneppen model. From left to right, the different lines refer to $\tau_w = 10^0$, 10^1, 10^2, 10^3, 10^4, 10^5, 10^6, 10^7 and 10^8, respectively, although the first four lines overlap. The apparent cut-off for small τ_w is purely the result of an optimization procedure employed to improve run times.

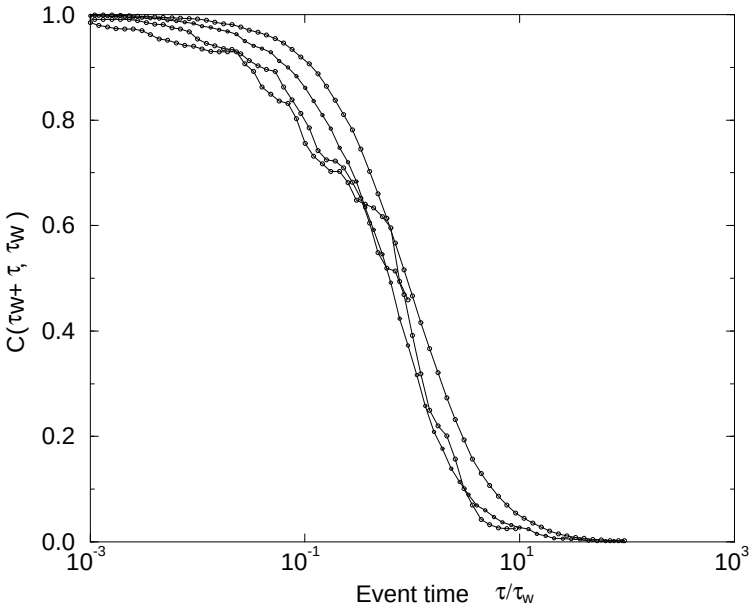

Figure 5. The same data as in figure 4 for $\tau_w \geqslant 10^5$, this time plotted against τ/τ_w, indicating partial collapse. From right to left (as viewed from the upper portion of the graph), the curves refer to $\tau_w = 10^5$, 10^6, 10^7 and 10^8, respectively.

where the critical exponent γ depends on the dimensionality. In low dimensions $\gamma > 1$, but $\gamma = 1$ in high dimensions where the scaling relations given by (18) and (19) break down. In this case the active site never remains localized in any one part of the system for any significant time and the following argument does not apply.

As before, let $C(\tau_w + \tau, \tau_w)$ be the proportion of the system that has not hopped between times τ_w and $\tau_w + \tau$. Clearly C will decrease when the avalanche jumps to a new part of the system. If we now coarse grain over length and timescales much larger than $\langle S \rangle$ and $\langle n_{cov} \rangle$, then, as consecutive avalanches are spatially uncorrelated, we can write the following continuous differential equation for C:

$$\frac{dC}{d\tau} \approx -\frac{C}{N}\frac{\langle n_{cov} \rangle}{\langle S \rangle}. \tag{20}$$

C only decays if the avalanche jumps to a part of the system it has not already visited, hence the factor of C on the right-hand side of (20). Furthermore, each avalanche changes a proportion $\langle n_{cov} \rangle / N$ of the system and lasts for a time $\langle S \rangle$, which accounts for the remaining factors. Integrating (20) from τ_w to $\tau_w + \tau$ with $C(\tau_w, \tau_w) = 1$ gives

$$C(\tau_w + \tau, \tau_w) \sim \left(1 + \frac{\tau}{\tau_w}\right)^{-\alpha} \tag{21}$$

where $\alpha = \lim_{\tau \to \infty}(\tau \langle n_{cov} \rangle)/(N \langle S \rangle)$. That $C(\tau_w + \tau, \tau_w)$ depends on τ and τ_w only through the ratio τ/τ_w demonstrates that the system ages. Although this derivation is sufficient to explain our simulation results, it is not clear that the coarse graining assumption is valid as $\tau \to \infty$, even for arbitrarily large systems. It is also not obvious if this procedure can be extended to account for the results of Boettcher and Paczuski [21, 22].

If indeed the Bak–Sneppen model *does* age in event time τ, this calls into question the usual assumption of stationarity in most previous studies of the Bak–Sneppen model, since an ageing system does not obey time-translational invariance and hence cannot be stationary. It is possible that previous studies have relied too heavily on one-time functions such as critical exponents etc., which may appear to tend to stationary values even when two-time functions are still evolving. This is a subtle question and further investigation would be desirable. Note that the ageing we have observed (apparent or otherwise) is *dimensional dependent*—it *only* holds in low dimensions, not in the mean field. Hence the assumption of stationarity in section 2.3 is still valid.

Turning now to consider avalanche time τ^{av}, the same coarse-graining assumptions lead to the following differential equation for $C(\tau_w^{av} + \tau^{av}, \tau_w^{av})$:

$$\frac{dC}{d\tau^{av}} \approx -\frac{C\langle n_{cov} \rangle}{N} \tag{22}$$

which differs from (20) by a factor of $\langle S \rangle$. This can be solved as before to give

$$C(\tau_w^{av} + \tau^{av}, \tau_w^{av}) \sim \exp\left\{-a\left(\frac{\tau_w^{av}}{N}\right)^{\frac{\gamma}{\gamma-1}}\left[\left(1 + \frac{\tau^{av}}{\tau_w^{av}}\right)^{\frac{\gamma}{\gamma-1}} - 1\right]\right\} \tag{23}$$

where a is an arbitrary constant. Since this expression tends to zero as $\tau_w^{av} \to \infty$ for all $\tau^{av} > 0$, we conclude that the system does *not* age in avalanche time. This may relate to the failure to observe ageing in the sandpile model [21], where a timescale similar to τ^{av} is usually employed. Note that this conclusion also holds in the mean field case $\gamma = 1$, although the form of (23) is different. The numerical plot of $C(\tau_w^{av} + \tau^{av}, \tau_w^{av})$ for a one-dimensional system is given in figure 6.

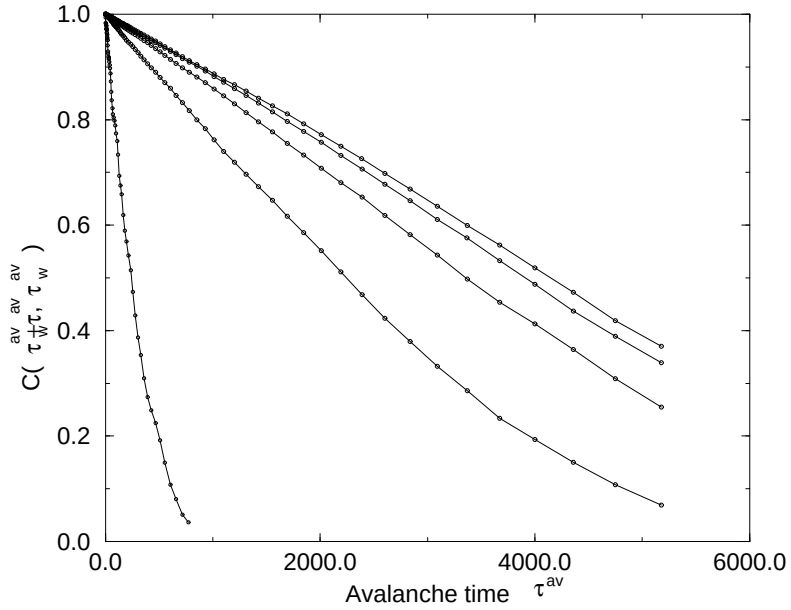

Figure 6. $C(\tau_w^{av} + \tau^{av}, \tau_w^{av})$ measured in avalanche time τ^{av} for a one-dimensional lattice with $N = 10^4$ sites in the $T = 0^+$ limit. From upper-right to lower-left, the curves refer to $\tau_w^{av} = R^6$, R^7, R^8, R^9 and R^{10}, respectively, where $R = 2.512$.

4. Conclusions

We have introduced the strongly interacting trap model, a version of Bouchaud's trap model which exhibits glassy behaviour for low temperatures and intermediate timeframes, but ultimately reaches stationarity as $t \to \infty$. In the limit of zero temperature the model becomes critical in all dimensions, including the mean field, so it has no 'lower critical dimension'.

A lattice version of the model was also introduced which appears to behave qualitatively similar to the mean field model in all the cases we have looked at, except one. This is the apparent ageing in the zero-temperature limit in low dimensions in what we have termed 'event time', which is absent in the mean field. This would represent a form of dimensional-dependent ageing, but is currently only supported by numerical evidence and hence remains somewhat speculative. It is also not clear at what dimension the ageing behaviour might start to break down.

Although this work was originally motivated by the range of spin glass models that have a critical point at $T = 0$, we do not claim any precise relationship between these systems and our model. We merely propose that our model may serve as a caricature of glass models with zero-temperature criticality, which, by its very simplicity, should allow for fuller analysis of this class of systems, both theoretically and numerically. It may also serve as a link between glass theory and models of self-organized criticality.

Acknowledgments

The author gratefully acknowledges many fruitful discussions with Mike Cates, Peter Sollich, Martin Evans, Mike Evans and Suzanne Fielding. This work was funded under EPSRC grant no GR/M09674.

Appendix A. Derivation of (7) and (8)

In this appendix we derive the expressions for ω_∞ quoted in (7) and (8) for non-integer and integer values of $x = T/b_0$, respectively. The steady state solution is found by substituting the form of $P_\infty(b)$ given by (6) into the definition of $\omega(t)$ given in (2). This results in the following integral equation for ω_∞:

$$\frac{1}{z+1} = \int_0^\infty \frac{\rho(b)}{z\omega_\infty \mathrm{e}^{b/T}+1}\,\mathrm{d}b. \tag{A.1}$$

Substituting $\rho(b) = \frac{1}{b_0}\mathrm{e}^{-b/b_0}$ and making the change of variables $u = \mathrm{e}^{-b/T}$ gives

$$\frac{1}{z+1} = x\int_0^1 \frac{u^x}{u+z\omega_\infty}\,\mathrm{d}u \tag{A.2}$$

$$= \frac{x}{z\omega_\infty(1+x)} F(1, 1+x; 2+x; -(z\omega_\infty)^{-1}). \tag{A.3}$$

For $z\omega_\infty < 1$ and non-integer x the hypergeometric function F can be rewritten as [23]

$$(z\omega_\infty)^{-1}F(1, 1+x; 2+x; -(z\omega_\infty)^{-1})$$

$$= \Gamma(2+x)\Gamma(-x)(z\omega_\infty)^x - x\frac{\Gamma(2+x)\Gamma(x)}{(\Gamma(1+x))^2}\sum_{k=0}^{\infty}\frac{(-z\omega_\infty)^k}{k-x} \tag{A.4}$$

where $\Gamma(x)$ is the usual gamma function. Inserting this into (A.3) gives the final expression (7), where use has been made of the identity

$$\Gamma(x)\Gamma(-x) = -\frac{\pi}{x\sin\pi x}. \tag{A.5}$$

The sum on the right-hand side of (A.4) is ill defined when x is an integer. In this case, an equivalent expression can be found, either by integrating (A.2) directly or by substituting $x = n \pm \varepsilon$ into (7) with n an integer, and letting $\varepsilon \to 0$. Both methods yield the same answer, given in (8).

Appendix B. Derivation of the $T = 0^+$ solution (12)

It is possible to derive, in a non-rigorous manner, explicit expressions for ω_∞ and $P_\infty(b)$ for arbitrary $\rho(b)$ in the limit $T \to 0^+$. The starting point is the same integral equation as in (A.1),

$$\frac{1}{z+1} = \int_0^\infty \frac{\rho(b)}{\mathrm{e}^{b/T+\ln(z\omega_\infty)}+1}\,\mathrm{d}b. \tag{B.1}$$

This imposes significant constraints on the allowed forms of ω_∞. For instance, if $T\ln(z\omega_\infty) \to 0$ as $T \to 0$, then (B.1) would imply the contradictory result $z = \infty$. Indeed, if one assumes that $\ln(z\omega_\infty) \sim T^\alpha$, then self-consistency of (B.1) demands that $\alpha = -1$ and therefore

$$\omega_\infty \sim \frac{1}{z}\mathrm{e}^{-b_\mathrm{c}/T} \tag{B.2}$$

where b_c is some arbitrary constant.

For $\ln(z\omega_\infty) = -b_\mathrm{c}/T$, the denominator inside the integral of (B.1) is essentially constant except around the region $b \approx b_\mathrm{c}$. Since $\rho(b)$ is independent of T, we can always choose T small enough so that $\rho(b)$ is slowly varying over this region, assuming that $\rho(b)$ is continuous at b_c. Hence the integral simplifies to

$$\frac{1}{z+1} = \int_0^{b_\mathrm{c}} \rho(b)\,\mathrm{d}b \tag{B.3}$$

which fixes b_c. Substituting (B.2) into the general expression for $P_\infty(b)$ given in (6) results in the final expression (12). To give some idea of typical values of b_c, a simple exponential prior $\rho(b) = \frac{1}{b_0} e^{-b/b_0}$ gives $b_c = b_0 \ln(1 + z^{-1})$, whereas $b_c = (1 + z)^{-1}$ when $\rho(b)$ is uniformly distributed on $[0, 1]$.

References

[1] Bouchaud J-P 1992 *J. Physique* I **2** 1705
[2] Monthus C and Bouchaud J-P 1996 *J. Phys. A: Math. Gen.* **29** 3847
[3] Sollich P, Lequeux F, Hébraud H and Cates M E 1997 *Phys. Rev. Lett.* **78** 2020
[4] Sollich P 1998 *Phys. Rev.* E **58** 1998
[5] Evans R M L, Cates M E and Sollich P 1999 *Eur. J. Phys.* B **10** 705
[6] Fielding S M, Sollich P and Cates M E 1999 *Preprint* cond-mat/9907101
[7] Newman C M and Stein D L 1994 *Phys. Rev. Lett.* **72** 2286
[8] Stein D L and Newman C M 1995 *Phys. Rev.* E **51** 5228
[9] Marinari E, Parisi G and Ruiz–Lorenzo J J 1998 *Spin Glasses and Random Fields* ed A P Young (Singapore: World Scientific)
[10] Pázmándi F, Zaránd G and Zimányi G T 1999 *Phys. Rev. Lett.* **83** 1034
(Pázmándi F, Zaránd G and Zimányi G T 1999 *Preprint* cont-mat/9902156)
[11] Bak P and Sneppen K 1993 *Phys. Rev. Lett.* **71** 4083
[12] Paczuski M, Maslov S and Bak P 1996 *Phys. Rev.* E **53** 414
[13] Bouchaud J-P, Comtet A and Monthus C 1995 *J. Physique* I **5** 1521
[14] Flyvbjerg H, Sneppen K and Bak P 1993 *Phys. Rev. Lett.* **71** 4087
[15] de Boer J, Derrida B, Flyvbjerg H, Jackson A D and Wettig T 1994 *Phys. Rev. Lett.* **73** 906
[16] Dickman R 1997 *Non-Equilibrium Statistical Mechanics in One Dimension* ed V Privman (Cambridge: Cambridge University Press)
[17] Head D A 1999 *J. Phys. A: Math. Gen.* submitted
[18] Jovanović B, Buldyrev S V, Havlin S and Stanley H E 1994 *Phys. Rev.* E **50** R2403
[19] Grassberger P 1995 *Phys. Lett.* A **200** 277
[20] Dhar D 1999 *Physica* A **263** 4
[21] Boettcher S and Paczuski M 1997 *Phys. Rev. Lett.* **79** 889
[22] Boettcher S 1997 *Phys. Rev.* E **56** 6466
[23] Prudnikov P A, Brychkov Y A and Marichev O I 1990 *Integrals and Series vol 3: More Special Functions* (New York: Gordon and Breach)